Anomalous transmission of phonons in superlattices at oblique propagation: an analysis based on finite difference equations

1997 J. Phys.: Condens. Matter 9 6791

(http://iopscience.iop.org/0953-8984/9/32/003)

J. Phys.: Condens. Matter **9** (1997) 6791–6804. Printed in the UK PII: S0953-8984(97)82545-3

Anomalous transmission of phonons in superlattices at oblique propagation: an analysis based on finite difference equations

Hatsuyoshi Kato† and Shin-ichiro Tamura‡

† Tomakomai National College of Technology, Nishikioka, Tomakomai 059-12, Japan
‡ Department of Applied Physics, Hokkaido University, Sapporo 060, Japan

Received 12 March 1997, in final form 28 May 1997

Abstract. Anomalous mode-converted transmission of phonons is studied based on the new formulas for the transmitted amplitudes of phonons propagating oblique to the layer interfaces of superlattices. A 2×2 transfer matrix which well describes the transmission of the coupled longitudinal and transverse phonons in an isotropic model is introduced. With the use of this transfer matrix we can derive finite difference equations which govern the transmitted amplitudes of both the longitudinal and transverse phonons. These equations can be solved exactly for periodic superlattices and approximately for certain aperiodic superlattices. The results are applied to the study of the unusual intermode oscillations in phonon transmission in both periodic superlattices and aperiodic superlattices with variable thickness of bilayers.

1. Introduction

Despite a great deal of work on the propagation of phonons in multilayered elastic media [1], there is still considerable interest in this topic. Specifically, we have recently reported an unusual behaviour of the transmission characteristic of phonons in a periodic superlattice (SL) at an oblique angle of propagation [2]. This can be seen in the vicinity of an anti-crossing frequency in the SL dispersion relation: the wave energy oscillates back and forth between the different polarizations as the wave propagates through the SL. These oscillations are analogous to the Pendellösung effect for electrons and to the Borrmann effect (the anomalous transmission effect) for x-rays [3, 4]. In the case of phonons in SLs, the reflected and transmitted beams correspond to the different acoustic phonon modes, i.e., transverse (T) and longitudinal (L) and the acoustic energy of the mode converted from the incident polarization steadily grows in spite of a small rate of mode conversion at each interface of layers.

These results have, for the most part, been analysed *numerically* based on the transfer matrix method. The relevant transfer matrix which describes the coupled longitudinal and transverse modes of phonons for oblique propagation is generally 6×6 for an anisotropic case and 4×4 in the isotropic approximation. The calculation of the transmission or reflection properties of phonons in a SL with a finite number of periods requires the multiplication of these matrices as many times as the number of periods. Thus the analytical calculation to obtain this product is not straightforward but rather seems to be almost hopeless even in the isotropic approximation [5]. Hence some different approach is required to analytically study the phonon transmission in the multilayered systems at oblique angles.

0953-8984/97/326791+14$19.50

In the present work we consider the isotropic model and introduce a tractable 2×2 transfer matrix rather than the 4×4 one which is valid in the frequency bands of phonons where the reflection rate is small. The results are particularly useful in getting physical insight into the resonant mode conversion of phonons, that is, the relevant quantities such as the conversion rate and associated period of oscillations can be derived analytically. A key idea is to neglect reflected amplitudes of phonons at the boundaries of unit periods but not those at the interface within a unit period. With this 2×2 transfer matrix we can derive finite difference equations which relate the transmitted amplitudes at the interfaces of three adjacent bilayers (for a given mode of phonons). These equations are solved exactly for a periodic superlattice and also approximately for an aperiodic superlattice with coherent hetero-interfaces for reflection and penetration (CHIRP SL) [6]. Figure 1 shows schematically a CHIRP SL consisting of alternating thin elastic layers of two different materials with gradually changing periodicity. The increment of the layer thickness ΔD is assumed to be common to both A and B constituent layers. This aperiodic SL has many attractive features for device application [6]. Although this structure is highly aperiodic, we see that phonons are transmitted perfectly for some range of frequency. Also the transmission rates in this structure oscillate in a way different from the resonant transmission we studied previously and the mode conversion between different phonon polarizations exhibits an interesting behaviour.

In the next section the transfer-matrix method is introduced and an approximated 2×2 transfer matrix which reproduces very well the exact results for phonon transmission is defined. In section 3 finite difference equations which relate the phonon amplitudes in the adjacent bilayers are derived and their exact solutions for periodic superlattices and approximate solutions for aperiodic superlattices are given. To see the validity of our results the formulas are applied to the resonant mode conversion of phonons in periodic superlattices and also aperiodic superlattices with layers of variable thickness. Section 4 summarizes the present work.

2. Transfer matrix

We consider the coupled transverse and longitudinal vibrations in the isotropic continuum approximation and write the displacement vector in the nth bilayer ($n \geqslant 1$) as follows:

$$\boldsymbol{u}_n^{(j)} = \sum_{J=T,L} \left\{ a_{J,n}^{(j)} \boldsymbol{e}_J^{(j)} \exp\left(\mathrm{i}k_J^{(j)} z_n^{(j)}\right) + b_{J,n}^{(j)} \tilde{\boldsymbol{e}}_J^{(j)} \exp\left(-\mathrm{i}k_J^{(j)} z_n^{(j)}\right) \right\} \mathrm{e}^{\mathrm{i}(k_\parallel x_\parallel - \omega t)} \qquad (j = \mathrm{A},\ \mathrm{B}) \tag{1}$$

where j discriminates the constituent materials A and B, $a_{J,n}^{(j)}$ and $b_{J,n}^{(j)}$ are the amplitudes of the transmitted and reflected phonons of mode J, respectively, $\boldsymbol{e}_J^{(j)}$ and $\tilde{\boldsymbol{e}}_J^{(j)}$ are the unit polarization vectors, $k_\parallel$ and $k_J^{(j)}$ are the wave numbers parallel and perpendicular to the interfaces, respectively, and ω is the angular frequency. The Cartesian coordinates are settled so that $x_\parallel$ and z axes are parallel and perpendicular to the interfaces (see figure 1) and the variable $z_n^{(A)} \equiv z - z_{n-1}$ ranges from 0 to $D_n^{(A)}$ and $z_n^{(B)} \equiv z - z_{n-1} - D_n^{(A)}$ ranges from 0 to $D_n^{(B)}$, where z_n ($z_0 = 0$) indicates the boundary between nth and $(n+1)$th bilayers, and $D_n^{(A)}$ and $D_n^{(B)}$ are the thicknesses of the A and B layers in the nth bilayer. Note that equation (1) is also valid in the substrate ($n = 0$) if we put $z_{-1} = -\infty$ and $j = \mathrm{B}$.

The transfer-matrix method is a useful way to obtain the transmission and reflection rates of phonons in SLs. For SLs consisting of crystalline layers with elastic anisotropy, the relevant transfer matrix is a 6×6 matrix, in general. In the present case, however, the

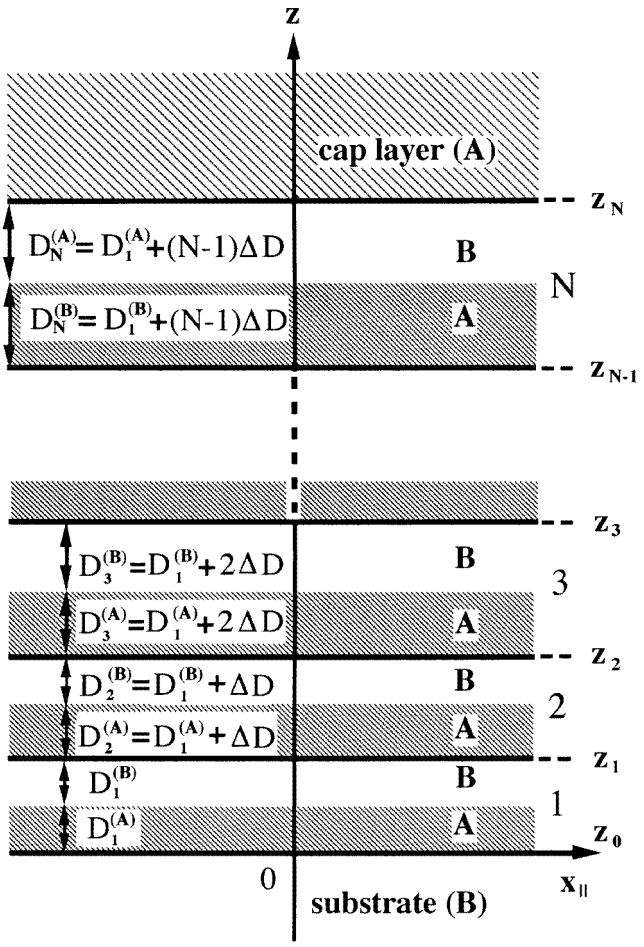

Figure 1. Schematic geometry of the finite superlattice with N bilayers. The thicknesses of the layers apply to both the periodic superlattice (with $\Delta D = 0$) and the aperiodic superlattice (with $\Delta D \neq 0$) for which the thickness of each constituent layer in a bilayer increases by ΔD with increasing number of bilayers. The substrate and cap layer are assumed to have the elastic properties of B and A layers, respectively.

transfer matrix is a 4×4 matrix because phonons we consider are mixed T and L modes in isotropic elastic media. The phonon amplitudes $a^{(j)}_{J,n+1}$ and $b^{(j)}_{J,n+1}$ in a bilayer are related to the ones in the previous bilayer $a^{(j)}_{J,n}$ and $b^{(j)}_{J,n}$ by multiplication by a transfer matrix. Explicitly,

$$\begin{bmatrix} a^{(j)}_{T,n+1} \\ a^{(j)}_{L,n+1} \\ b^{(j)}_{T,n+1} \\ b^{(j)}_{L,n+1} \end{bmatrix} = F^{(j)}_n \begin{bmatrix} a^{(j)}_{T,n} \\ a^{(j)}_{L,n} \\ b^{(j)}_{T,n} \\ b^{(j)}_{L,n} \end{bmatrix} \qquad (n \geqslant 0) \tag{2}$$

where the transfer matrix $F^{(j)}_n$ is given by

$$F^{(j)}_n = \Phi^{(j)}_n f^{(jk)} \Phi^{(k)}_n f^{(kj)} \qquad (j = \text{A and } k = \text{B}, \text{ or } j = \text{B and } k = \text{A}) \tag{3}$$

$$\Phi_n^{(j)} = \begin{bmatrix} \exp(\mathrm{i}k_T^{(j)} D_n^{(j)}) & 0 & 0 & 0 \\ 0 & \exp(\mathrm{i}k_L^{(j)} D_n^{(j)}) & 0 & 0 \\ 0 & 0 & \exp(-\mathrm{i}k_T^{(j)} D_n^{(j)}) & 0 \\ 0 & 0 & 0 & \exp(-\mathrm{i}k_L^{(j)} D_n^{(j)}) \end{bmatrix} \tag{4}$$

$$f^{(kj)} = \left[M^{(k)}\right]^{-1} M^{(j)} \tag{5}$$

$$M^{(j)} = \begin{bmatrix} \cos\phi_T & \sin\phi_L & -\cos\phi_T & \sin\phi_L \\ -\sin\phi_T & \cos\phi_L & -\sin\phi_T & -\cos\phi_L \\ c_{44}\frac{\cos 2\phi_T}{\sin\phi_T} & 2c_{44}\cos\phi_L & c_{44}\frac{\cos 2\phi_T}{\sin\phi_T} & -2c_{44}\cos\phi_L \\ -2c_{44}\cos\phi_T & c_{11}\frac{\cos 2\phi_T}{\sin\phi_L} & 2c_{44}\cos\phi_T & c_{11}\frac{\cos 2\phi_T}{\sin\phi_L} \end{bmatrix}. \tag{6}$$

In these expressions $\Phi_n^{(j)}$ represents the phase change of phonons associated with the propagation of the distance $D_n^{(j)}$, ϕ_J is the angle of transmission or reflection of the phonon mode J, and c_{11} and c_{44} are the stiffness constants. On the r.h.s. of equation (6), we have omitted the superscript j from ϕ_T, ϕ_L, c_{11}, and c_{44}, for simplicity. From equation (5), we note that the matrix $f^{(jk)}$ satisfies

$$f^{(kj)} = \left[f^{(jk)}\right]^{-1}. \tag{7}$$

This matrix $f^{(jk)}$ consists of the amplitude transmission and reflection coefficients at a single interface for a phonon incident on the j layer from the k layer.

The formulation based on the 4×4 transfer matrix given above is still intractable for analytical calculations. Accordingly, we develop an approximate formula for the transmission of phonons which utilizes the matrices of 2×2 rather than of 4×4. The amplitudes we keep here are those of the transmitted phonons, i.e., a_T and a_L. Thus, equations (3) and (4) become for $j = \mathrm{B}$ and $k = \mathrm{A}$ (hereafter we omit the superscript j from the 2×2 transfer matrix $\hat{F}$)

$$\hat{F}_n = \hat{\Phi}_n^{(B)} \hat{f}^{(BA)} \hat{\Phi}_n^{(A)} \hat{f}^{(AB)} \tag{8}$$

$$\hat{\Phi}_n^{(j)} = \begin{bmatrix} \exp(\mathrm{i}k_T^{(j)} D_n^{(j)}) & 0 \\ 0 & \exp(\mathrm{i}k_L^{(j)} D_n^{(j)}) \end{bmatrix} \tag{9}$$

where

$$\hat{f}^{(jk)} = \begin{bmatrix} [f^{(jk)}]_{11} & [f^{(jk)}]_{12} \\ [f^{(jk)}]_{21} & [f^{(jk)}]_{22} \end{bmatrix}. \tag{10}$$

In this approximation, we should note that the 2×2 matrix $\hat{f}^{(jk)}$ consists of the elements of the original 4×4 matrix $f^{(jk)}$, but is *not* defined by equation (6) with matrix $M^{(j)}$ simply reduced to 2×2. This means that we neglect reflected amplitudes $b_{J,n}^{(j)}$ of phonons at the boundaries of unit periods but *not* those at the interface within a unit period. A crucial point is that we require that the same relation as equation (7) holds for the reduced matrix $\hat{f}^{(kj)}$, i.e.,

$$\hat{f}^{(kj)} = \left[\hat{f}^{(jk)}\right]^{-1} \tag{11}$$

or this equation defines $\hat{f}^{(kj)}$. Here we note that the transfer matrix $\hat{F}_n$ satisfies $|\det[\hat{F}_n]| = 1$ but not $\det[\hat{F}_n] = 1$, in general, whereas the original 4×4 transfer matrix F_n satisfies $\det[F_n] = 1$.

With these matrices defined, equation (2) is reduced to

$$\begin{bmatrix} a_{T,n+1} \\ a_{L,n+1} \end{bmatrix} = \hat{F}_n \begin{bmatrix} a_{T,n} \\ a_{L,n} \end{bmatrix} \tag{12}$$

where the amplitudes $a_{T,n}$ and $a_{L,n}$ are those in the B layer (we also omit the superscripts of $a_{T,n}$ and $a_{L,n}$, hereafter). The validity of the present approximation will be seen in the next section.

3. Finite difference equations

In order to find equations satisfied by the transmitted amplitudes of T and L phonons we need an additional equation which relates the amplitudes $a_{J,n+2}$ with $a_{J,n+1}$, i.e.,

$$\begin{bmatrix} a_{T,n+2} \\ a_{L,n+2} \end{bmatrix} = \hat{F}_{n+1} \begin{bmatrix} a_{T,n+1} \\ a_{L,n+1} \end{bmatrix} \tag{13}$$

where the transfer matrix $\hat{F}_{n+1}$ is obtained from $\hat{F}_n$ by replacing the layer thickness $D_n^{(j)}$ with $D_{n+1}^{(j)}$. In the following we develop the formula applicable to two cases, i.e., an aperiodic CHIRP SL with $D_{n+1}^{(j)} = D_n^{(j)} + \Delta D$, ($j$ = A and B) and a periodic SL with $D_{n+1}^{(j)} = D_n^{(j)}$.

Using equations (12) and (13), we obtain two difference equations satisfied by the amplitudes of both phonon modes

$$a_{T,n+2} - \left(\hat{F}'_{11} + \hat{F}_{22}\frac{\hat{F}'_{12}}{\hat{F}_{12}}\right)a_{T,n+1} + \left(\hat{F}_{11}\hat{F}_{22}\frac{\hat{F}'_{12}}{\hat{F}_{12}} - \hat{F}'_{12}\hat{F}_{21}\right)a_{T,n} = 0 \tag{14}$$

$$a_{L,n+2} - \left(\hat{F}_{11}\frac{\hat{F}'_{21}}{\hat{F}_{21}} + \hat{F}'_{22}\right)a_{L,n+1} + \left(\hat{F}_{11}\hat{F}_{22}\frac{\hat{F}'_{21}}{\hat{F}_{21}} - \hat{F}_{12}\hat{F}'_{21}\right)a_{L,n} = 0. \tag{15}$$

In these equations we have written $[\hat{F}_n]_{ij} = \hat{F}_{ij}$ and $[\hat{F}_{n+1}]_{ij} = \hat{F}'_{ij}$ to save the indices. In equation (14) we approximate the small off-diagonal elements $\hat{F}'_{12}$ and $\hat{F}'_{21}$ which describe the mode-converted transmission by $\hat{F}_{12}$, and $\hat{F}_{21}$, respectively. This approximation is exact for periodic SLs and also a good approximation for the CHIRP SL as shown below. Thus, equations (14) and (15) are summarized as

$$a_{J,n+2} - 2\tau_{J,n}a_{J,n+1} + \delta_n a_{J,n} = 0 \tag{16}$$

where J = T and L, and

$$\tau_{T,n} = \tfrac{1}{2}\left([\hat{F}_{n+1}]_{11} + [\hat{F}_n]_{22}\right) \tag{17}$$

$$\tau_{L,n} = \tfrac{1}{2}\left([\hat{F}_n]_{11} + [\hat{F}_{n+1}]_{22}\right) \tag{18}$$

$$\delta_n \quad = \det[\hat{F}_n]. \tag{19}$$

The explicit expression of $\tau_{J,n}$ is complicated (see appendix A) but δ_n is simply given by

$$\delta_n = \exp\left\{\mathrm{i}\left[\left(k_T^{(A)} + k_L^{(A)}\right)D_n^{(A)} + \left(k_T^{(B)} + k_L^{(B)}\right)D_n^{(B)}\right]\right\}. \tag{20}$$

Hence, we write

$$\delta_n = \mathrm{e}^{\mathrm{i}(2\alpha + 2\beta n)} \tag{21}$$

where α and β are real constants. Equation (16) thus can be written as

$$a_{J,n+2} - 2\mathrm{e}^{\mathrm{i}(\alpha+\beta n)}\varepsilon_{J,n}a_{J,n+1} + \mathrm{e}^{\mathrm{i}(2\alpha+2\beta n)}a_{J,n} = 0 \tag{22}$$

where $\varepsilon_{J,n}$ (J = T and L) are defined by

$$\tau_{J,n} \equiv \varepsilon_{J,n}\mathrm{e}^{\mathrm{i}(\alpha+\beta n)}. \tag{23}$$

We now consider two cases:

3.1. Periodic SLs with $D_n^{(A)} = D_n^{(B)} = D_0/2$

In a periodic SL $\Delta D = 0$ ($\beta = 0$) and $\hat{F}_n$ does not depend on n, so $\hat{F}_n \equiv \hat{F}$. In addition $\tau_{L,n} = \tau_{T,n} \equiv \tau$ and $\delta_n \equiv \delta = \mathrm{e}^{2\mathrm{i}\alpha}$ with $2\alpha = (k_T^{(A)} + k_L^{(A)} + k_T^{(B)} + k_L^{(B)})D_0/2$ and D_0 is the periodicity. Under these conditions it is readily seen that equation (22) has the following analytical solutions

$$a_{T,n} = X_1\lambda_1^n + X_2\lambda_2^n \tag{24}$$

$$a_{L,n} = Y_1\lambda_1^n + Y_2\lambda_2^n \tag{25}$$

where λ_1 and λ_2 are the eigenvalues of the matrix $\hat{F}$, i.e.,

$$\left.\begin{matrix}\lambda_1\\ \lambda_2\end{matrix}\right\} = \tau \pm \sqrt{\tau^2 - \delta} \tag{26}$$

and the expressions of X_i and Y_i ($i = 1, 2$) are given in appendix B.

Introducing a variable θ defined by

$$\cosh\theta \equiv \tau\delta^{-1/2} \tag{27}$$

or equivalently

$$\left.\begin{matrix}\lambda_1\\ \lambda_2\end{matrix}\right\} = \left.\begin{matrix}\mathrm{e}^{\mathrm{i}\alpha+\theta}\\ \mathrm{e}^{\mathrm{i}\alpha-\theta}\end{matrix}\right\} \tag{28}$$

the solutions (24) and (25) can be rewritten as

$$a_{J,n} = \frac{\mathrm{e}^{\mathrm{i}n\alpha}}{\sinh\theta}\{-a_{J,0}\sinh(n-1)\theta + a_{J,1}\mathrm{e}^{-\mathrm{i}\alpha}\sinh n\theta\}. \tag{29}$$

For an L phonon incidence $a_{L,0} = 1$ and $a_{T,0} = 0$ ($a_{T,0}$ and $a_{L,0}$ are the amplitudes of the T and L phonons in the substrate) and $a_{L,1} = \hat{F}_{22}$ and $a_{T,1} = \hat{F}_{12}$. Thus, equation (29) gives

$$|a_{T,n}|^2 = |\hat{F}_{12}|^2\left|\frac{\sinh n\theta}{\sinh\theta}\right|^2 \tag{30}$$

$$|a_{L,n}|^2 = \left|\frac{-\sinh(n-1)\theta + \hat{F}_{22}\mathrm{e}^{-\mathrm{i}\alpha}\sinh n\theta}{\sinh\theta}\right|^2. \tag{31}$$

The transmission rate t of phonons is defined by the transmitted acoustic Poynting vector normalized by the incident acoustic flux. If we measure the transmitted flux at the B layer with the same elastic properties as the substrate, we find for the L phonon incidence

$$t_{T,n} = \left|\frac{a_{T,n}}{a_{L,0}}\right|^2 Z_{LT} \tag{32}$$

$$t_{L,n} = \left|\frac{a_{L,n}}{a_{L,0}}\right|^2 \tag{33}$$

where $Z_{LT} = \sin 2\phi_T/\sin 2\phi_L$ and ϕ_T and ϕ_L refer to the angles in the B layer.

We now apply the above formulas to the frequency regime where the resonant mode conversion between the L and T polarizations occurs in a periodic superlattice. The resonant mode conversion happens at frequencies for which the L branch of the dispersion curves in the folded Brillouin zone attempts to overtake the T branch because of the larger velocity of the longitudinal wave. Actually the coupling of the L and T polarizations leads to the repulsion of the dispersion curves and the anticrossing behaviour (see figure 2). The condition of the resonance is given by

$$(k_T^{(A)} + k_T^{(B)})D_0/2 = (k_L^{(A)} + k_L^{(B)})D_0/2 + 2m\pi \equiv \chi \tag{34}$$

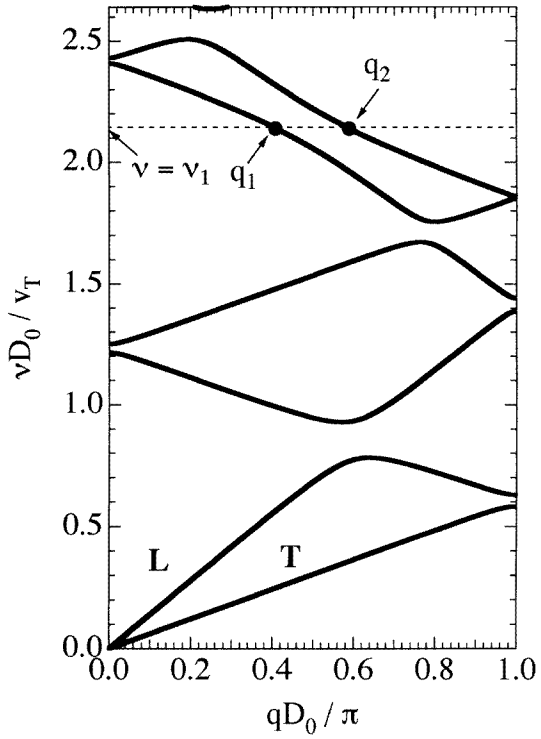

Figure 2. Dispersion relations of the coupled longitudinal (L) and transverse (T) modes in a periodic GaAs/AlAs superlattice in the isotropic continuum approximation. The thicknesses $D_n^{(A)}$ of A layer (AlAs) and $D_n^{(B)}$ of B layer (GaAs) are the same (the periodicity is $D_0 = D_n^{(A)} + D_n^{(B)}$ with $D_n^{(A)} = D_n^{(B)}$) and v_T is the transverse sound velocity in GaAs. The numerical values of the sound velocities are 5.03 $\times 10^5$ cm s^{-1} and 5.98 $\times 10^5$ cm s^{-1} (L modes) and 3.03 $\times 10^5$ cm s^{-1} and 3.60 $\times 10^5$ cm s^{-1} (T modes) for GaAs and AlAs, respectively, and the mass densities are 5.36 g cm^{-3} for GaAs and 3.76 g cm^{-3} for AlAs. The propagation direction of the L (T) mode is 45° (25.2°) in the GaAs layers and 56.9° (30.4°) in the AlAs layers. The lowest anticrossing frequency is denoted by ν_1 and q_1 and q_2 are the wave numbers of the two propagating eigenwaves at $\nu = \nu_1$.

or equivalently

$$q_1 - q_2 = mG_0 \tag{35}$$

where m is an integer, $G_0 = 2\pi/D_0$ is the magnitude of the reciprocal superlattice vector, and q_1 and q_2 are the wave numbers of the envelope functions of the mixed T and L phonons.

At the resonance $\delta = \mathrm{e}^{2\mathrm{i}\chi - 2m\pi\mathrm{i}}$ and τ takes a simple form as given by

$$\tau = \mathrm{e}^{\mathrm{i}\chi}\varepsilon_0 \tag{36}$$

$$\varepsilon_0 = \frac{f_{11}^{(AB)} f_{22}^{(AB)} - f_{12}^{(AB)} f_{21}^{(AB)} \cos\xi}{f_{11}^{(AB)} f_{22}^{(AB)} - f_{12}^{(AB)} f_{21}^{(AB)}} \tag{37}$$

where $\xi = (k_T^{(A)} - k_L^{(A)})D_0/2$ or $\xi = (k_T^{(B)} - k_L^{(B)})D_0/2$. From equation (27) we find

$$\cosh\theta = \cosh\theta_0 \equiv (-1)^m \varepsilon_0. \tag{38}$$

Here we note that ε_0 is real and positive because the matrix elements $f_{12}^{(AB)}$ and $f_{21}^{(AB)}$ which express the intermode transmission at a layer interface are smaller than the elements $f_{11}^{(AB)}$ and $f_{22}^{(AB)}$ describing the intramode transmission of phonons. Furthermore, the explicit expressions of $f_{ij}^{(AB)}$ show that the product $f_{11}^{(AB)} f_{22}^{(AB)}$ is positive and $f_{12}^{(AB)} f_{21}^{(AB)}$ is negative (see appendix A), so the modulus of ε_0 is smaller than unity ($\varepsilon_0 = 0.960$ in the example below). Hence, θ_0 is pure imaginary, i.e.,

$$\theta_0 = \mathrm{i}\cos^{-1}\left[(-1)^m \varepsilon_0\right]. \tag{39}$$

Thus the equations (30) and (31) tell us that the transmission rates oscillate with the propagation distance and the period n_0 of the oscillation between L and T polarizations is given by

$$n_0 = \frac{\pi}{\cos^{-1}\varepsilon_0}. \tag{40}$$

With the expressions derived above, we have plotted in figure 3 the transmission rates of phonons for L phonon incidence and see how the transmitted energy is converted to the T phonons with the number of bilayers. In this numerical example the materials for A and B layers are AlAs and GaAs, respectively, and the incident angle of the L (T) phonon in the GaAs layer is 45° (25.2°) and the frequency ν_1 which satisfies $\nu_1 D_0/v_T = 2.15$ (v_T is the transverse sound velocity in GaAs) is chosen (see figure 2). The bold line indicates the result derived from equation (30) which coincides well with the dots calculated with the exact 4×4 transfer matrix. The period of oscillation deduced from equation (40) is $n_0 = 11.02$. This value also agrees with the period of the mode-converted transmission shown in figure 3.

Equation (30) can be interpreted more physically as follows. For most values of the frequency ν, there exist two propagating superlattice modes whose frequency matches that of the incident wave. Let us denote the wave numbers of these modes by q_1 and q_2. Provided that these two wave numbers are far removed from points at which anti-crossing occurs, one of these modes will have essentially the character of an L wave and the other a T wave. Then the incident L wave will excite the L wave with a large amplitude and the T wave with a much smaller amplitude and vice versa. However, for an incident frequency in the vicinity of an anti-crossing frequency ν_1 in figure 2, for instance, the difference between the wave numbers q_1 and q_2 is small and beats occur by the interference between the two transmitted eigenwaves $\exp(\mathrm{i}q_1 D_0)$ and $\exp(\mathrm{i}q_2 D_0)$ of the system. This means that equation (30) should be equivalent to

$$\left|a_{T,n}\right|^2 = \left|\hat{F}_{12}\right|^2 \frac{\sin^2[n(q_1 - q_2)D_0/2]}{\sin^2[(q_1 - q_2)D_0/2]} \tag{41}$$

that is, $\theta = \mathrm{i}(q_1 - q_2)D_0/2$ and $\cos[(q_1 - q_2)D_0/2] = \varepsilon_0$. After the waves have propagated a number of bilayers n such that $|q_1 - q_2|nD_0 = \pi$ the waves will combine so the L components cancel and the T components add. This corresponds to the distance for complete energy transfer to T polarization. Therefore the energy returns to the L wave after travelling n_0 bilayers, where

$$n_0 = \frac{2\pi}{|q_1 - q_2|D_0}. \tag{42}$$

It follows from these considerations that the transmission rate of the T component of the wave varies as $t_{T,n} \sim \sin^2(\pi n/n_0)/\sin^2(\pi/n_0)$ and the transmission rate of the L component varies as $t_{L,n} \sim \cos^2(\pi n/n_0)/\sin^2(\pi/n_0)$. This explains the oscillations in the transmission rate exhibited in figure 3.

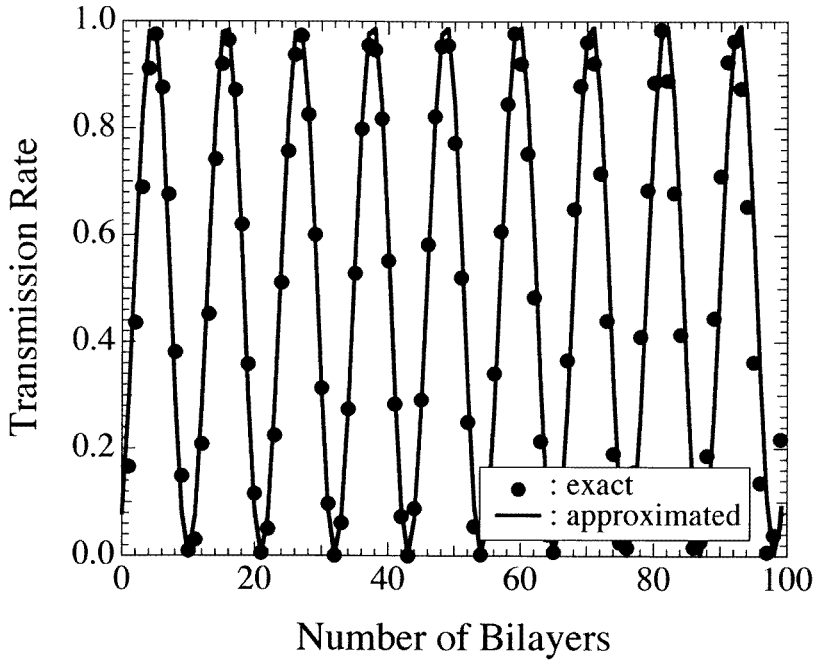

Figure 3. Transmission rate of transverse (T) phonons versus number of bilayers in a periodic GaAs/AlAs superlattice. The solid line is the calculation with the approximated 2×2 transfer matrix or equivalently with the solution of the finite differential equation and the dots are the exact results based on the 4×4 transfer matrix. Longitudinal phonon incidence is assumed and the frequency chosen is $\nu = \nu_1$ at which the condition for the resonant mode conversion is satisfied, i.e., $\nu_1 D_0/v_T = 2.15$. The other parameters are the same as in figure 2.

3.2. Aperiodic case with $\Delta D \neq 0$

We consider an aperiodic CHIRP SL shown in figure 1, where the layer thickness increases by a small amount ΔD, or $D_{n+1}^{(j)} = D_n^{(j)} + \Delta D$ (j = A and B). In this case the coefficients α and β are given by

$$2\alpha = (k_T^{(A)} + k_T^{(B)} + k_L^{(A)} + k_L^{(B)})(D_0/2 - M\Delta D) \tag{43}$$

$$2\beta = (k_T^{(A)} + k_T^{(B)} + k_L^{(A)} + k_L^{(B)})\Delta D. \tag{44}$$

In equation (43) $M = N/2$ (N is the total number of bilayers) and we have chosen $D_M^{(A)} = D_M^{(B)} = D_0/2$, or $2\nu_1 D_M^{(A)}/v_T = 2\nu_1 D_M^{(B)}/v_T = \nu_1 D_0/v_T = 2.15$. This is a condition that the resonant mode conversion occurs in the corresponding periodic superlattice. Figure 4 shows the transmission rate of T phonons versus the number of bilayers obtained by numerically solving the finite difference equation (22) (solid line) together with the exact results (dots) obtained from the original 4×4 transfer matrix. Here the A and B layers are again AlAs and GaAs, respectively, and the total number of bilayers is $N = 2M = 100$. In addition we have chosen $\nu_1 \Delta D/v_T = 2.15 \times 10^{-3}$ or $2\Delta D/D_0 = 0.002$. Both the magnitude and period of the oscillations are reproduced very well as for the case of the periodic SL considered above and this again validates equation (22) based on the 2×2 transfer matrix we derived. The inset also exhibits the L phonon transmission rate obtained by solving the difference equation (22) for J = L, which varies as $t_{T,n} + t_{L,n} = 1$ is satisfied.

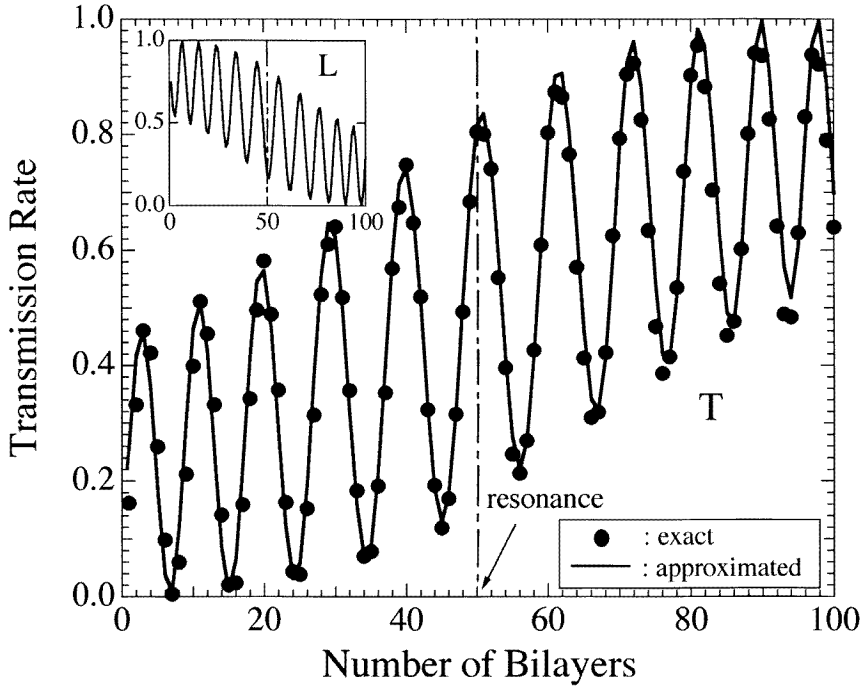

Figure 4. Transmission rate of transverse (T) phonons versus number of bilayers in a CHIRP (coherent hetero-interfaces for reflection and penetration) superlattice consisting of AlAs (A) and GaAs (B) layers. The incident phonon is longitudinal (L) polarization and the angle of incidence in the GaAs substrate is 45°. The dots are the exact results calculated with the 4×4 transfer matrix and the solid line shows the transmission rates calculated by solving numerically the finite difference equation. The inset shows the transmission rate of L phonons calculated by solving the finite difference equation. This figure is for $\nu_1 \Delta D/v_T = 2.15 \times 10^{-3}$ and $2\nu_1 D_M^{(A)}/v_T = 2\nu_1 D_M^{(B)}/v_T = 2.15$ ($= \nu_1 D_0/v_T$ with v_T the transverse sound velocity in GaAs) at the Mth ($M = 50$) bilayer, i.e., the resonance layer of the superlattice.

Now the characteristic behaviours of the transmission rates shown in figure 4 can be understood as follows. Suppose, for example, the L wave is incident on a superlattice that has a repeat distance such that the resonance condition for buildup of a T wave is *not* satisfied at the front of the structure. If the repeat distance slowly increases with distance into the superlattice, a region will eventually be reached in which the conversion condition is satisfied. In this region the energy in the wave will oscillate back and forth between the L and T polarizations.

Unfortunately, it is not straightforward to solve analytically the finite difference equation (22) for this aperiodic structure. Here we give only an approximate solution which is found heuristically, i.e.,

$$a_{J,n} = \left(X_{J,1} \prod_{k=1}^{n} \rho_{J,k-1} + X_{J,2} \prod_{k=1}^{n} \sigma_{J,k-1} \right) \exp\left[\mathrm{i}\left(\alpha - \frac{3}{2}\beta \right) n + \frac{\mathrm{i}}{2}\beta n^2 \right] \qquad (n \geqslant 1) \quad (45)$$

where

$$\left.\begin{matrix} \rho_{J,n} \\ \sigma_{J,n} \end{matrix}\right\} = \varepsilon_{J,n} \pm \left(\varepsilon_{J,n}^2 - \mathrm{e}^{\mathrm{i}\beta} \right)^{1/2} \qquad (46)$$

and the expressions of the coefficients $X_{J,1}$ and $X_{J,2}$ are given in appendix B.

In these equations $\rho_{J,n}$ and $\sigma_{J,n}$ are the solutions of

$$x_n^2 - 2\varepsilon_{J,n}x_n + \mathrm{e}^{\mathrm{i}\beta} = 0. \tag{47}$$

The amplitude (45) becomes the exact solution of equation (22) if $\rho_{J,n}$ and $\sigma_{J,n}$ are the solutions of

$$x_{n+1}x_n - 2\varepsilon_{J,n}x_n + \mathrm{e}^{\mathrm{i}\beta} = 0. \tag{48}$$

Again for an L phonon incidence, i.e., $a_{T,0} = 0$ and $a_{L,0} = 1$, equation (45) leads to the squared amplitude of T phonons in the nth bilayer as

$$\begin{aligned}\left|a_{T,n}\right|^2 &= \left|\frac{\hat{F}_{12}}{\rho_{T,0} - \sigma_{T,0}}\right|^2 \left[\prod_{k=1}^{n}\left|\rho_{T,k-1}\right|^2 + \prod_{k=1}^{n}\left|\sigma_{T,k-1}\right|^2 - 2\,\mathrm{Re}\Big(\prod_{k=1}^{n}\rho_{T,k-1}\sigma_{T,k-1}^{*}\Big)\right] \\ &= \left|\frac{\hat{F}_{12}}{\rho_{T,0} - \sigma_{T,0}}\right|^2 \left\{\prod_{k=1}^{n}\left|\rho_{T,k-1}\right|^2 + \prod_{k=1}^{n}\left|\sigma_{T,k-1}\right|^2 \right. \\ &\quad \left. -2\cos\left[\sum_{k=1}^{n}(\varphi_{T,k-1} - \psi_{T,k-1})\right]\right\}\end{aligned} \tag{49}$$

where $\varphi_{T,k}$ and $\psi_{T,k}$ are the phases of $\rho_{T,k}$ and $\sigma_{T,k}$, respectively, and we have used the fact that $|\rho_{J,k}||\sigma_{J,k}| = 1$. The transmission rate of T phonons derived from equation (49) has also been plotted in figure 5(a) by a bold line. The parameters assumed for this figure are the same as those for figure 4. Here we note that the sum of the first and second terms in the parenthesis grows with increasing n and the third term oscillates with respect to n. However, under the present approximation the amplitude of the oscillation is independent of n. Although the values of the local extrema of the approximated and exact transmission rates do not coincide, the periods of the oscillation (which depend on the distance from the substrate and change locally) agree very well. More precisely, for a small variation of the phase difference $\varphi_{T,k} - \psi_{T,k}$ with respect to k we can define the local period $\tilde{n}$ of the oscillation at the nth bilayer as

$$\tilde{n} = \frac{2\pi}{|\varphi_{T,n} - \psi_{T,n}|} = \frac{\pi}{\cos^{-1}|\varepsilon_{T,n}|} \tag{50}$$

where we have used the fact that the phase of $\varepsilon_{T,n}$ is very close to π and neglected its small imaginary part (note that $\varepsilon_{T,n}$ is real at the resonance layer $n = M$ if $\tau_{T,n} = \mathrm{Tr}[\hat{F}_n]/2$, see equation (17)). The periods of oscillations are plotted in figure 5(b) for comparison. Dots are estimated from figure 4 and the solid line is the local period $\tilde{n}$. The period of oscillations $\tilde{n}$ becomes maximum at the resonance layer.

4. Summary

In this article we have given an approximated formula for determining the transmission amplitudes of the coupled L and T phonons propagating obliquely in a superlattice. This is done in the isotropic model by deriving finite difference equations based on the transfer matrices approximated to be 2×2 from the original ones of 4×4. The formula derived has been applied to the periodic SL, specifically to the frequencies for which the resonant mode conversion between different phonon polarizations occurs. The calculated transmission rates coincide well with the exact numerical results for both the magnitude and period of oscillations that are characteristic of the mode-converted transmission.

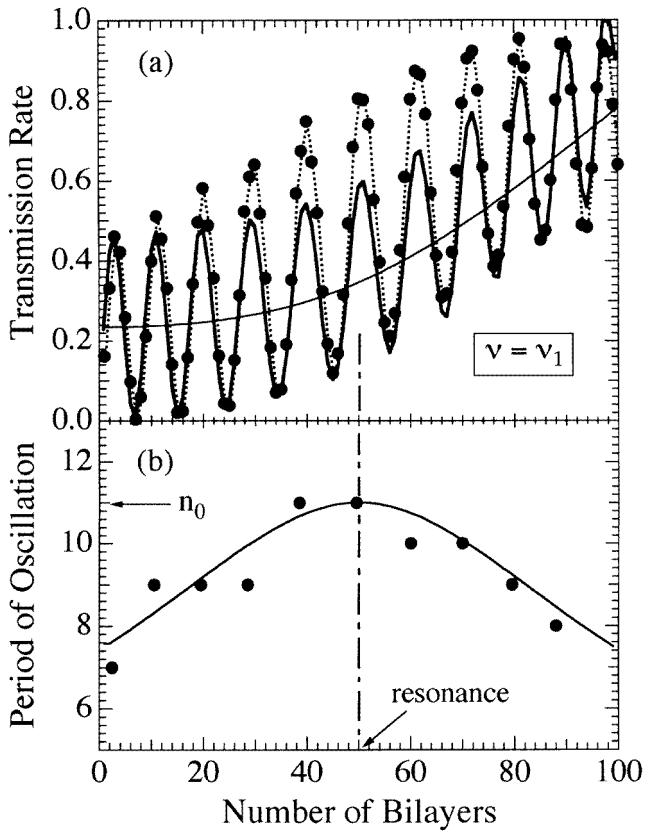

Figure 5. (a) Transmission rate of transverse (T) phonons versus number of bilayers in a CHIRP superlattice. The bold line is calculated from the approximated solution (49) of the finite difference equation and the thin line shows the mean values obtained by neglecting the last term of equation (49). The dots connected by a dotted line are the exact results calculated from the 4×4 transfer matrix (the same as the dots in figure 4). The conditions and parameters assumed are the same as in figure 4. (b) Period of oscillations of the T phonon transmission rate. The solid line is calculated from an approximated formula (50) and the dots are the values estimated from the numerical transmission rate shown in figure 4. $n_0 = 11.02$ is the period of the oscillations in the periodic superlattice with $D_n^{(A)} = D_n^{(B)} = D_0/2$ (figure 3).

Our formula has also been applied to an aperiodic SL called the CHIRP SL for which the period slowly increases (or decreases) with distance. Although the finite difference equations give the results which reproduce the exact transmission rates quantitatively, the approximate solutions that we found heuristically explain the transmission rates only semiquantitatively. For the CHIRP structure we consider, there should be better approximate solutions of the finite difference equations than the ones described in the present work. It would be an interesting mathematical problem to find such a solution.

Another interesting aperiodic multilayered system studied recently is the graded-composition multi-quantum well which can be used for optoelectronic devices [7, 8]. In these structures the thickness of the B layer changes according to $D_n^{(B)} = (n - 0.5)D_{AB}^2/L_s$ ($n = 1, 2, \ldots, L_s/D_{AB}$), where D_{AB} is the thickness of a bilayer and L_s is the system size. The transmission and associated mode conversion of phonons propagating in these

structures can also be analysed by the formulas derived in the present work.

It should be noted that the formulas obtained here are valid in the frequency bands of phonons where the reflection rate of phonons is small. For oblique phonon propagation there also exist the frequency regions where the transmission rates of both L and T phonons are small. Such simultaneous frequency gaps of both L and T phonons can be seen to be distributed quite widely in the ν–$k_{\parallel}$ plane of periodic superlattices [5, 9]. Hence in these frequency regions there should be similar approximate formulas valid for the reflected amplitudes of phonons, which can be used to analyse the intermode Bragg reflections [10–14]. The study on this topic will appear elsewhere.

Finally, we remark that in the real anisotropic superlattices the anomalous mode-converted transmission of phonons is more complicated due to the coupling to both transverse modes of phonons. In this case the mode conversion between two transverse modes are also possible in addition to the mode conversions from the longitudinal to two transverse modes and vice versa. However, as far as we are concerned with the phonon propagation in a saggital plane with mirror symmetry, the resonant mode conversion only between the longitudinal mode and single transverse branch as studied in the present work is possible.

Acknowledgments

We thank H J Maris for helpful discussions. This work has been supported in part by the Murata Science Foundation.

Appendix A.

The explicit expressions for the diagonal elements of the transfer matrix $\hat{F}_n$ are given by

$$\left[\hat{F}_n\right]_{11} = \exp\left(\mathrm{i}k_T^{(B)} D_n^{(B)}\right)\left[f_{11}^{(AB)} f_{22}^{(AB)} \exp\left(\mathrm{i}k_T^{(A)} D_n^{(A)}\right) - f_{12}^{(AB)} f_{21}^{(AB)} \exp\left(\mathrm{i}k_L^{(A)} D_n^{(A)}\right)\right]\Big/ d \tag{A1}$$

$$\left[\hat{F}_n\right]_{22} = \exp\left(\mathrm{i}k_L^{(B)} D_n^{(B)}\right)\left[f_{11}^{(AB)} f_{22}^{(AB)} \exp\left(\mathrm{i}k_L^{(A)} D_n^{(A)}\right) - f_{12}^{(AB)} f_{21}^{(AB)} \exp\left(\mathrm{i}k_T^{(A)} D_n^{(A)}\right)\right]\Big/ d \tag{A2}$$

where

$$d = f_{11}^{(AB)} f_{22}^{(AB)} - f_{12}^{(AB)} f_{21}^{(AB)}. \tag{A3}$$

If we assume that A and B layers are different only in their mass densities (elastic constants are the same), the expressions of $f_{ij}^{(AB)}$ take the simple forms

$$f_{11}^{(AB)} = \left(\sin 2\phi_T^{(A)} + \sin 2\phi_T^{(B)}\right)\Big/ 4\cos\phi_T^{(A)} \sin\phi_T^{(B)} \tag{A4}$$

$$f_{12}^{(AB)} = \kappa\left(\cos 2\phi_T^{(A)} - \cos 2\phi_T^{(B)}\right)\Big/ 4\cos\phi_T^{(A)} \sin\phi_L^{(B)} \tag{A5}$$

$$f_{21}^{(AB)} = -\left(\cos 2\phi_T^{(A)} - \cos 2\phi_T^{(B)}\right)\Big/ 4\cos\phi_L^{(A)} \sin\phi_T^{(B)} \tag{A6}$$

$$f_{22}^{(AB)} = \left(\sin 2\phi_L^{(A)} + \sin 2\phi_L^{(B)}\right)\Big/ 4\cos\phi_L^{(A)} \sin\phi_L^{(B)} \tag{A7}$$

where $\kappa = \sin^2\phi_L^{(A)}/\sin^2\phi_T^{(A)} = \sin^2\phi_L^{(B)}/\sin^2\phi_T^{(B)}$.

Appendix B.

The coefficients X_i and Y_i $(i = 1, 2)$ of equations (24) and (25) are given by

$$X_1 = \frac{(\hat{F}_{11} - \lambda_2)a_{T,0} + \hat{F}_{12}a_{L,0}}{\lambda_1 - \lambda_2} \tag{B1}$$

$$X_2 = \frac{(\lambda_1 - \hat{F}_{11})a_{T,0} - \hat{F}_{12}a_{L,0}}{\lambda_1 - \lambda_2} \tag{B2}$$

$$Y_1 = \frac{(\hat{F}_{22} - \lambda_2)a_{L,0} + \hat{F}_{21}a_{T,0}}{\lambda_1 - \lambda_2} \tag{B3}$$

$$Y_2 = \frac{(\lambda_1 - \hat{F}_{22})a_{L,0} - \hat{F}_{21}a_{T,0}}{\lambda_1 - \lambda_2}. \tag{B4}$$

In the above equations (B1)–(B4) $a_{T,0}$ and $a_{L,0}$ are the amplitudes of the T and L phonons in the substrate. Also the coefficients $X_{J,1}$ and $X_{J,2}$ of equation (45) are given by

$$X_{J,1} = \frac{a_{J,1} - \tilde{\sigma}_J a_{J,0}}{\tilde{\rho}_J - \tilde{\sigma}_J} \tag{B5}$$

$$X_{J,2} = \frac{\tilde{\rho}_J a_{J,0} - a_{J,1}}{\tilde{\rho}_J - \tilde{\sigma}_J} \tag{B6}$$

where $a_{J,0}$ is the amplitude of the J-mode phonon in the substrate and

$$\left.\begin{matrix}\tilde{\rho}_J \\ \tilde{\sigma}_J\end{matrix}\right\} = \left.\begin{matrix}\rho_{J,0} \\ \sigma_{J,0}\end{matrix}\right\} \mathrm{e}^{\mathrm{i}(\alpha-\beta)}. \tag{B7}$$

References

[1] See, for example, Cottam M G and Tilley D R 1989 *Introduction to Surface and Superlattice Excitations* (Cambridge: Cambridge University Press)
[2] Kato H, Maris H J and Tamura S 1996 *Phys. Rev.* B **53** 7884
[3] Howie A and Whelan M J 1961 *Proc. R. Soc.* A **263** 217
[4] Kato N 1963 *Acta Crystallogr.* **16** 276
Kato N 1961 *Acta Crystallogr.* **14** 526
Warren B E 1969 *X-ray Diffraction* (New York: Addison-Wesley) p 339
[5] Djafari-Rouhani B, Dobrzynski L, Dupark O H, Camley R E and Maradudin A A 1983 *Phys. Rev.* B **28** 1711
[6] Nakagawa T, Kawai N J, Ohta K and Kawashima M 1983 *Electron. Lett.* **19** 822
[7] Mathine D L, Maracas G N, Gerber D S and Droopad R 1994 *J. Appl. Phys.* **75** 4551
[8] Vlaev S, Garcia-Moliner F and Velasco V R 1995 *Phys Rev.* B **52** 13 784
[9] Sapriel J and Rouhani B D 1989 *Surf. Sci. Rep.* **10** 189
[10] Tamura S and Wolfe J P 1987 *Phys. Rev.* B **35** 2528
[11] Hurley D C, Tamura S, Wolfe J P and Morkoc H 1987 *Phys. Rev. Lett.* **58** 2446
[12] Tamura S, Hurley D C and Wolfe J P 1988 *Phys. Rev.* B **38** 1427
[13] Santos P V, Mebert J, Koblinger O and Ley L 1987 *Phys. Rev.* B **36** 1306
[14] Calle F, Cardona M, Richter E and Strauch D 1989 *Solid State Commun.* **72** 1153